Clinical and Experimental Medicine (2025) 25:99
https://doi.org/10.1007/s10238-025-01619-w

RESEARCH

YY1-induced transcription of AKR1C3 activates the Hedgehog signalling pathway to enhance lenalidomide resistance and glycolytic activity in multiple myeloma cells

Yang Chen[1] · Aijia Zhang[1] · Yuan Wang[2] · Daoda Qi[1] · Chengyi Peng[1] · Zihao Liang[2] · Jingjing Guo[1] · Yan Gu[1]

Received: 26 November 2024 / Accepted: 26 February 2025

Abstract

Lenalidomide (LEN) is a mainstay for treating multiple myeloma (MM), but its efficacy is often limited by resistance. We investigated the interaction between aldo–keto reductase family 1 member C3 (AKR1C3) and Yin Yang 1 (YY1) and their roles in LEN resistance. We induced LEN-resistant MM cell lines (H929R and U266R). Loss- or gain-of-function assays of AKR1C3 and YY1 were used to analyse the half maximal inhibitory concentration (IC_{50}) values, cell senescence, DNA damage, and glycolytic activity under LEN treatment. Chromatin immunoprecipitation was used to determine the interaction between YY1 and AKR1C3. As results, AKR1C3 and YY1 were upregulated in H929R and U266R cells. AKR1C3 silencing decreased the LEN's IC_{50}, slowed cell growth, enhanced senescence and DNA damage, reduced metabolic reprogramming. YY1 activated the transcription of AKR1C3 by binding to its promoter region. Similarly, silencing YY1 enhanced LEN sensitivity, suppressed glycolysis, and was counteracted by AKR1C3 overexpression. Mechanistically, YY1-AKR1C3 activated the Hedgehog pathway; fluticasone reversed the effects of AKR1C3 silencing on LEN resistance and glycolysis in H929R and U266R cells. Overall, YY1 activates AKR1C3 transcription and the Hedgehog pathway to increase LEN resistance and glycolytic activity in MM cells.

Keywords Multiple myeloma · Lenalidomide resistance · YY1 · AKR1C3 · Hedgehog pathway · Glycolysis

Introduction

Multiple myeloma (MM) is the second most common haematological malignancy, with an estimated 187,774 new diagnoses according to global cancer statistics in 2022 [1]. As an incurable and heterogeneous disease, MM arises from uncontrolled proliferation of monoclonal plasma cells in the bone marrow, leading to the overproduction of nonfunctional intact immunoglobulins or immunoglobulin chains [2] and ultimately causing dysfunction of major organs [3]. MM cells can release angiogenesis-related proteins [4] and recruit/activate inflammatory cells [5]; these alterations in the tumour bone marrow (BM) microenvironment lead to angiogenesis and immunosuppression [6].

Lenalidomide (LEN), a first-line immunomodulatory imide drug (IMiD), is preferred as a mainstay for treating MM [7, 8]. Its therapeutic effects are mediated through multiple mechanisms [9], including suppression of proinflammatory cytokines to inhibit myeloid cell-mediated inflammation [10], expansion of natural killer (NK) cell and T cell populations, and enhancement of cytotoxicity [11–13]. Although combination of IMiDs with other drugs, such as proteasome inhibitors, antibodies, and corticosteroids, can induce remission in most patients, but MM relapses in almost all patients due to acquired resistance of MM cells [8, 14]. IMiD resistance involves various molecular cascades or pathways [15]. To date, key mechanisms of LEN resistance include CRBN downregulation, cell surface marker alterations, Wnt/β-catenin pathway upregulation, and epigenetic modifications. Additional mechanisms such as CDK6

Yang Chen, Aijia Zhang and Yuan Wang have contributed equally to this work.

✉ Jingjing Guo
guojingjing0017@126.com

✉ Yan Gu
guyan703@foxmail.com

[1] Department of Geriatrics, The Second Hospital of Nanjing, Affiliated to Nanjing University of Chinese Medicine, Nanjing, People's Republic of China

[2] Clinical Research Center, The Second Hospital of Nanjing, Affiliated to Nanjing University of Chinese Medicine, Nanjing, People's Republic of China

Published online: 29 March 2025

overexpression, c-MYC activation, MEK-ERK pathway hyperactivation, proinflammatory cytokine secretion, extracellular vesicle release, and enhanced adhesion also warrant further investigation [16]. AKR1C3, a key enzyme in androgen biosynthesis, functions as an oncogenic driver by promoting tumour cell proliferation, invasion, and metastasis, which is associated with poor prognosis and reduced overall survival in cancer patients [17]. This enzyme catalyses diverse substrates, including carbohydrates, lipids, and steroids [18]. Notably, AKR1C3 endows hepatocellular carcinoma cells with adaptability to targeted therapy by regulating lipid droplet formation and glycolysis [19]. Metabolic reprogramming is a hallmark of cancer and involves alterations in glucose, glutamine, and lipid metabolism, enabling tumour cells to thrive in hostile microenvironments and sustain rapid growth [20]. A central feature is the Warburg effect, whereby cancer cells preferentially utilize aerobic glycolysis over mitochondrial oxidative phosphorylation for energy production, as evidenced by elevated glucose uptake and lactate secretion even under normoxic conditions [21–23]. This metabolic shift, driven by oncogenes and tumour suppressors, affects the expression and activity of various enzymes [24]. The Warburg effect also occurs in MM cells, ensuring their proliferation, growth, survival, and immune evasion, consequently leading to drug resistance and uncontrolled disease progression [25]. However, whether AKR1C3 is associated with glycolysis and LEN resistance in MM cells remains unclear and requires experimental validation.

YY1 is a transcription factor belonging to the GLI-Krüppel class of zinc finger proteins [26]. Depending on its cofactors, YY1 functions as either a transcriptional activator or a repressor [27, 28]. Widely expressed in mammals, YY1 regulates cellular proliferation, differentiation, and tumorigenesis [29]. Notably, YY1 upregulation enhances chemo- and immunoresistance in cancer cells by promoting the transcription of antiapoptotic genes [30]. In MM, the YY1-induced lncRNA TUG1 upregulates YOD1 expression to reduce bortezomib sensitivity [31]. However, the exact functions of YY1 in LEN resistance in MM has not been elucidated.

This study aims to investigate the functional interplay between YY1 and AKR1C3, specifically their roles in mediating LEN resistance and glycolysis in MM.

Materials and methods

Cell culture

The human MM cell lines U266 and H929 were obtained from the American Type Culture Collection (ATCC), verified through short tandem repeat profiling, confirmed to be free of mycoplasma contamination, and then cultured in RPMI-1640 medium (Thermo Fisher Scientific) supplemented with 20% fetal bovine serum (FBS) and 1% penicillin/streptomycin inside an incubator at 37 °C with 5% CO_2.

Artificial gene modification in cells

AKR1C3 (NM_001253908.2) or YY1 (NM_003403.5) was amplified, cloned, and inserted into the lentiviral vector pCDH-CMV-MCS-EF1-Pur (Solarbio), which was named AKR1C3 or YY1. The empty vector pCDH-CMV-MCS-EF1-Pur served as a negative control (Emp). Double-stranded oligos (ds-oligos) of AKR1C3 or YY1-specific short hairpin RNA (shRNA) sequences (Table 1) were cloned and inserted into the pLenti-shRNA-GFP-puro lentiviral vector (Asia-Vector Biotechnology), and the resulting recombinant plasmids were named AKR1C3-kd and YY1-kd. The nonspecific pLenti-shRNA-GFP-puro lentiviral vector was used as a negative control (Scr). The lentiviral vectors were cotransfected with the packaging plasmid psPAX2 (#12,260; Addgene) and pMD2. G (#12,259; Addgene) into 293 T cells at a 3:3:1 ratio (2.5 μg of lentiviral vector, 2.5 μg of psPAX2, and 0.83 μg of pMD2. G) using Lipofectamine (Thermo Fisher Scientific). Viral supernatants were harvested after 48 h, filtered and administered to the MM cell lines at a multiplicity of infection (MOI) of 80 for 24 h. Transduced cells were subsequently selected in complete medium containing 1 μg/ml puromycin for 7 days and maintained for subsequent experiments.

Table 1 shRNA sequences

Symbol	Ds Oligos
AKR1C3-sh#1	5′-GAAACATTTGCTAGCCAGCTGTTCAAGAGACAGCTGGCTAGCAAATGTTTCTTTTTT-3′
AKR1C3-sh#2	5′-TGACAGTGATGGATTCAAAACTTCAAGAGAGTTTTGAATCCATCACTGTCATTTTTT-3′
AKR1C3-sh#3	5′-GGTTCCGCCATATAGATTCTGTTCAAGAGACAGAATCTATATGGCGGAACCTTTTTT-3′
YY1-sh#1	5′-GGAAGCAAGAUGGCCCUUCATTCAAGAGATGAAGGGCCAUCUUGCUUCCTTTTTT-3′
YY1-sh#2	5′-GAUGCUUGCCAUGUAUUUCATTCAAGAGATGAAAUACAUGGCAAGCAUCTTTTTT-3′
YY1-sh#3	5′-GCAUUCUGUCAUCAGGAUAATTCAAGAGAUUAUCCUGAUGACAGAAUGCTTTTTT-3′

Reverse transcription quantitative polymerase chain reaction (RT−qPCR)

Total RNA was extracted from cells via FreeZol Reagent (R711-01, Vazyme), and cDNA was synthesized with the PrimeScript RT reagent kit (R233, Vazyme). qPCR analysis was performed using SYBR Premix Ex Taq (Q311, Vazyme). Relative gene expression, normalized to the reference gene GAPDH, was determined via the $2^{-\Delta\Delta CT}$ method. Primer sequences are listed in Table 2.

Western blot (WB) analysis

Total protein was extracted from cells via radioimmunoprecipitation assay lysis buffer (P0013B, Beyotime). Protein levels were determined via a BCA kit (P0010, Beyotime), the protein samples were separated via 12% SDS−PAGE and transferred onto nitrocellulose membranes (Bio-Rad Laboratories). The membranes were then blocked with 5% nonfat milk at room temperature for 30 min and incubated overnight at 4 °C with primary antibodies (Table 3). The next day, the membranes were incubated with HRP-conjugated anti-mouse/rabbit IgG secondary antibodies for 2 h at 25 °C. The signal was developed via an enhanced chemiluminescence (ECL) Plus (P0018S, Thermo Fisher Scientific). Protein quantification was conducted via ImageJ 1.48u software.

Cell counting kit-8 (CCK-8) assay

The viability of the MM cells was evaluated via a CCK-8 kit (C0038, Beyotime). Briefly, MM cells were suspended at a concentration of 1×10^5 cells/mL, seeded into 96-well plates, and treated with LEN at concentrations of 0.00, 0.01, 0.10, 1.00, 5.00, 10.00, 100.00, and 1000.00 μM at 37 °C for 1 h. Subsequently, 10 μL of CCK-8 reagent was added to each well, and the cells were incubated at 37 °C for 4 h. The optical density was measured at 450 nm via a microplate reader.

Table 3 Antibodies

Target	Catalogue	Company
AKR1C3	PA5-28,065	Thermofisher
HK2	#2867	CST
GLUT1	#MA5-31,960	Thermofisher
LDHA	#PA5-27,406	Thermofisher
GLI1	#2553	CST
PTCH1	#2468	CST
HIP1	#8226	CST
YY1	ab109237	abcam
ACTB	#MA1-140	Thermofisher
gamma-H2AX	A700-053	Thermofisher
CEBPA	ab317442	abcam
PKM2	#4053	CST
ATF4	Ab85049	abcam

5-Ethynyl-2′-deoxyuridine (EdU) labelling assay

Following the instructions of the EdU labelling kit (C0071S, Beyotime), MM cells were incubated with the EdU working solution for 2 h and then fixed with 4% paraformaldehyde at room temperature for 15 min. Afterward, the cells were incubated with 0.3% Triton X-100 at room temperature for 15 min. Apollo staining solution was then added, and the cells were incubated in the dark at room temperature for 30 min. Nuclei were stained with 4′,6-diamidino-2-phenylindole (DAPI) for 5 min, and the slides were mounted for observation under a fluorescence microscope.

Table 2 Primers

Symbol	Forward	Reverse
AKR1C3	5′-GTGATCAAGGATGATCGAGGAG-3′	5′-GAGGATCTGCCGACTGTTGAT-3′
HK2	5′-TGCCCGCTTTGAGAGAGTTT-3′	5′-TGTGACGATGTTGGCTTGAG-3′
GLUT1	5′-CTTTGTGGCCTTCTTTGAAGTG-3′	5′-CATTGTAGGACAGCCAGGAC-3′
LDHA	5′-ATGGCAACTCTAAAGGATCAGC-3′	5′-GCGTTGCTCAGAGATTCCAA-3′
GLI1	5′-CTCCAGGACTGGCTGACTG-3′	5′-CTGTGCTGGGTTGTTGCTG-3′
PTCH1	5′-TGGATGAGCCACAAAGTGGA-3′	5′-TGGACTGGAACCTGAAGCTG-3′
HIP1	5′-GCACCGTGATGTTTGACCTA-3′	5′-GTGCACACCTTCAGTGTTG-3′
ACTB	5′-AGAGCTACGAGCTGCCTGAC-3′	5′-AGCACTGTGTTGGCGTACAG-3′
AKR1C3-promo#1- ChIP−qPCR	5′-GCTGAGGTTGAGGTTGAGGA-3′	5′-CCAGGTGAGGTAGAGGAGGA-3′
AKR1C3-promo#2- ChIP−qPCR	5′-GAGGTGAGGTGAGGAAGGAG-3′	5′-GGAGGAGGAAGGAGGTGAGG-3′
AKR1C3-promo#3- ChIP−qPCR	5′-GAGGTTGAGGTTGAGGTTGAG-3′	5′-GGTGAGGAAGGAGGAGGTGAG-3′

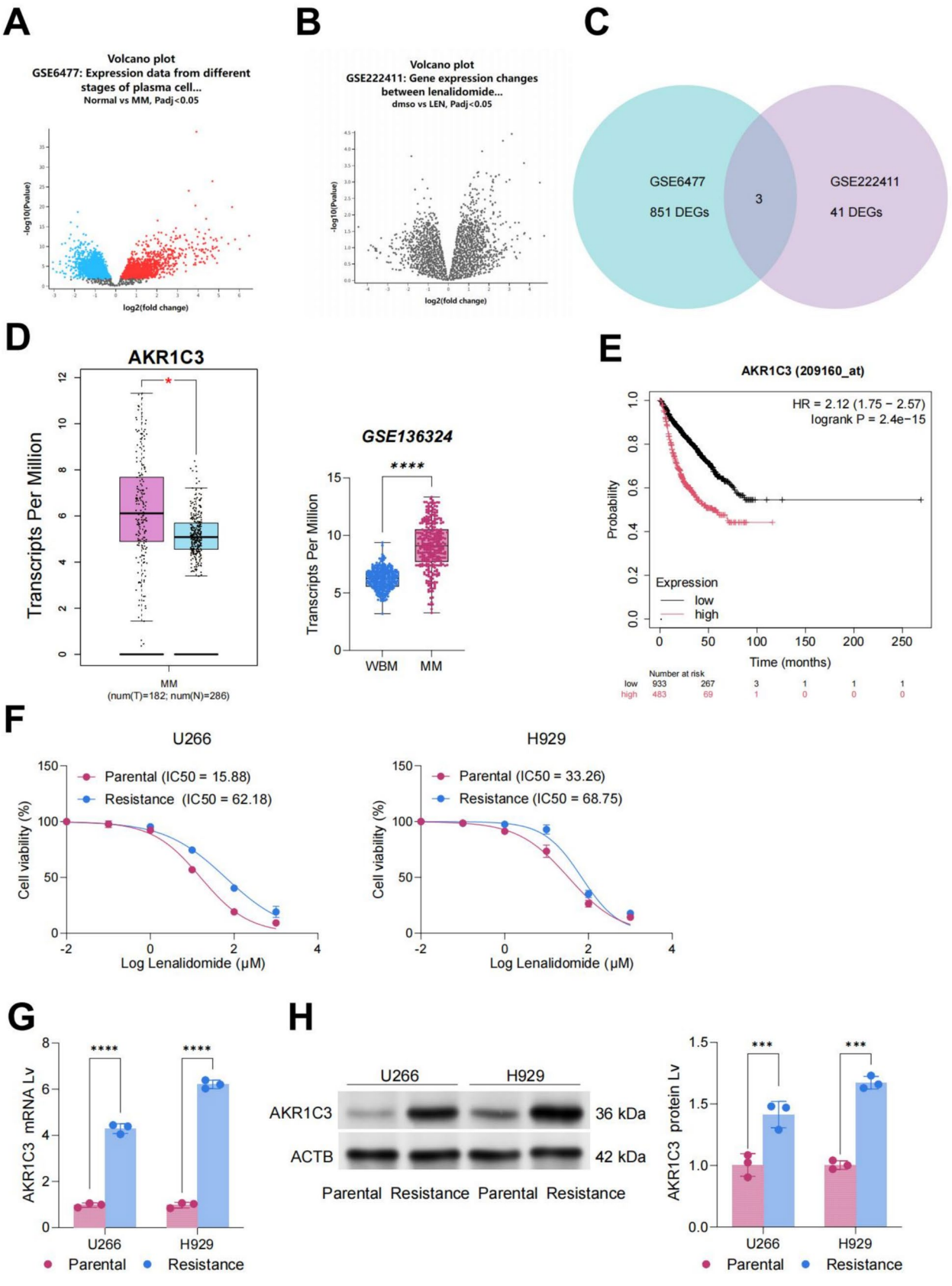
A
Volcano plot
GSE6477: Expression data from different stages of plasma cell...
Normal vs MM, Padj<0.05
-log10(Pvalue)
log2(fold change)
B
Volcano plot
GSE222411: Gene expression changes between lenalidomide...
dmso vs LEN, Padj<0.05
-log10(Pvalue)
log2(fold change)
C
GSE6477
851 DEGs
3
GSE222411
41 DEGs
D
AKR1C3
Transcripts Per Million
MM
(num(T)=182; num(N)=286)
GSE136324
****
Transcripts Per Million
WBM
MM
E
AKR1C3 (209160_at)
HR = 2.12 (1.75 − 2.57)
logrank P = 2.4e−15
Probability
Expression
low
high
Time (months)
Number at risk
low 933 267 3 1 1 1
high 483 69 1 0 0 0
F
U266
Parental (IC50 = 15.88)
Resistance (IC50 = 62.18)
Cell viability (%)
Log Lenalidomide (μM)
H929
Parental (IC50 = 33.26)
Resistance (IC50 = 68.75)
Cell viability (%)
Log Lenalidomide (μM)
G
AKR1C3 mRNA Lv
****
****
U266
H929
Parental
Resistance
H
U266
H929
AKR1C3
36 kDa
ACTB
42 kDa
Parental Resistance Parental Resistance
AKR1C3 protein Lv
***
***
U266
H929
Parental
Resistance

◂**Fig. 1** AKR1C3 is upregulated in LEN-resistant MM cells. **A**, Screening of significantly aberrantly expressed genes in MM via the GEO dataset GSE6477. **B** Analysis of aberrantly expressed genes in LEN-resistant MM samples via the GEO dataset GSE222411. **C** Venn diagram showing the intersection between genes from datasets GSE6477 and GSE222411 and the top three genes. **D** Expression levels of AKR1C3 in MM patients were analysed via data from The Cancer Genome Atlas (TCGA). **E** Significant correlation between high AKR1C3 expression and poor prognosis in MM patients according to the GSE136324 dataset. **F** Comparison of LEN IC_{50} values between parental MM cell lines (H929 and U266) and LEN-resistant cell lines (H929R and U266R) analysed via a CCK-8 assay (n = 6). **G** Relative mRNA expression levels of AKR1C3 in H929R and U266R cells compared with those in parental cell lines, as determined via RT−qPCR (n = 3). **H** Protein levels of AKR1C3 in H929R and U266R cells compared with those in parental cell lines, as determined by WB (n = 3). Differences were analysed using the Student's *t* tests. The bar graphs present the means ± SDs of independent replicate experiments. $^{**}p < 0.01$, $^{***}p < 0.001$, $^{****}p < 0.0001$

Colony formation assay

After reaching 70%–80% confluence, the cells were collected to obtain a single-cell suspension. The cell suspension was seeded into six-well plates with each well. Following a 14-d incubation, the cells were fixed for 10 min and stained with 0.5% crystal violet for 5 min. Colonies were counted under a microscope.

Senescence-associated beta-galactosidase (SABG) staining

Beta-galactosidase staining was employed to assess the extent of senescence in MM cells following irradiation. The experimental protocol followed the instructions provided with the beta-galactosidase staining kit (40754ES60, Yeasen).

Immunofluorescence staining

The cells were plated on sterile glass slides, cultured for 48 h, fixed with 4% paraformaldehyde for 15 min, permeabilized with 0.25% Triton-X 100 for 10 min, and blocked with 5% normal goat serum for 1 h. Immunofluorescence staining was performed with primary antibodies (Table 3). After being washed with phosphate-buffered saline (PBS), the cells were incubated with Alexa Fluor 488- or Alexa Fluor 546-conjugated secondary antibodies (Life Technologies). After nuclear staining with DAPI, the cells were observed under a microscope.

ATP production assessment

ATP levels were assessed via an ATP assay kit (S0026, Beyotime) according to the manufacturer's instructions. The cells were cultured in 12-well plates for 24 h, harvested with 200 µL of lysis buffer, and centrifuged at 12,000 × g for 5 min at 4 °C. Then, the supernatant was mixed with the detection solution. ATP concentrations were then analysed via a fluorescence spectrophotometer.

Glucose consumption and lactate production

The cells were cultured in the plates, upon reaching optimal assay density, the cells were exposed to low-glucose (5 mM) medium for 4 h, followed by glucose-free medium for 30 min and then glucose-free medium supplemented with 2.5 µg/mL 2-NBDG (ST2078, Beyotime) for another 30 min. Afterward, the cells were washed with PBS and harvested, and their fluorescence was measured via flow cytometry. Lactate production was quantified via a lactate colorimetric/fluorometric assay kit (K607-100, BioVision) according to the manufacturer's instructions. First, the cells were cultured in six-well plates in complete medium for 24 h. Subsequently, the medium was replaced with fresh medium containing 5 mM glucose, and the cells were further cultured for 15 h. The activity of lactic dehydrogenase (LDH) was measured via a human LDH ELISA kit (Enzyme-linked) according to the manufacturer's specifications.

Cell metabolic analysis

An XF24 extracellular flux analyser (Agilent Technologies) was used to analyse glycolysis and oxidative phosphorylation. The cells were seeded in XF24 plates at a density of 1.2×10^4 cells/well to reach optimal assay density. First, the cells were incubated in experimental medium at 37 °C for 1 h for baseline measurements. Various compounds prepared in the experimental medium were then added to each well. The extracellular acidification rate (ECAR) and oxygen consumption rate (OCR) were measured. The ECAR was reported as mpH/min and normalized to the protein concentration, whereas the OCR was reported as pmol/min and normalized to the protein concentration. Upon completion of the experiment, the cells were immediately collected, and the percentage in each well was normalized to the protein concentration.

Chromatin immunoprecipitation (ChIP)-qPCR

ChIP was performed using a ChIP assay kit (Millipore Corp) following the manufacturer's instructions. Briefly, 3×10^7 MM cells per sample were crosslinked with 1% formaldehyde in culture medium for 10 min at room temperature. The crosslinking process was terminated by adding glycine to a final concentration of 125 mM (5-min incubation). After lysis and sonication, 1% of the soluble chromatin fraction was decrosslinked at 4 °C overnight and served as Input control. The remaining chromatin was immunoprecipitated

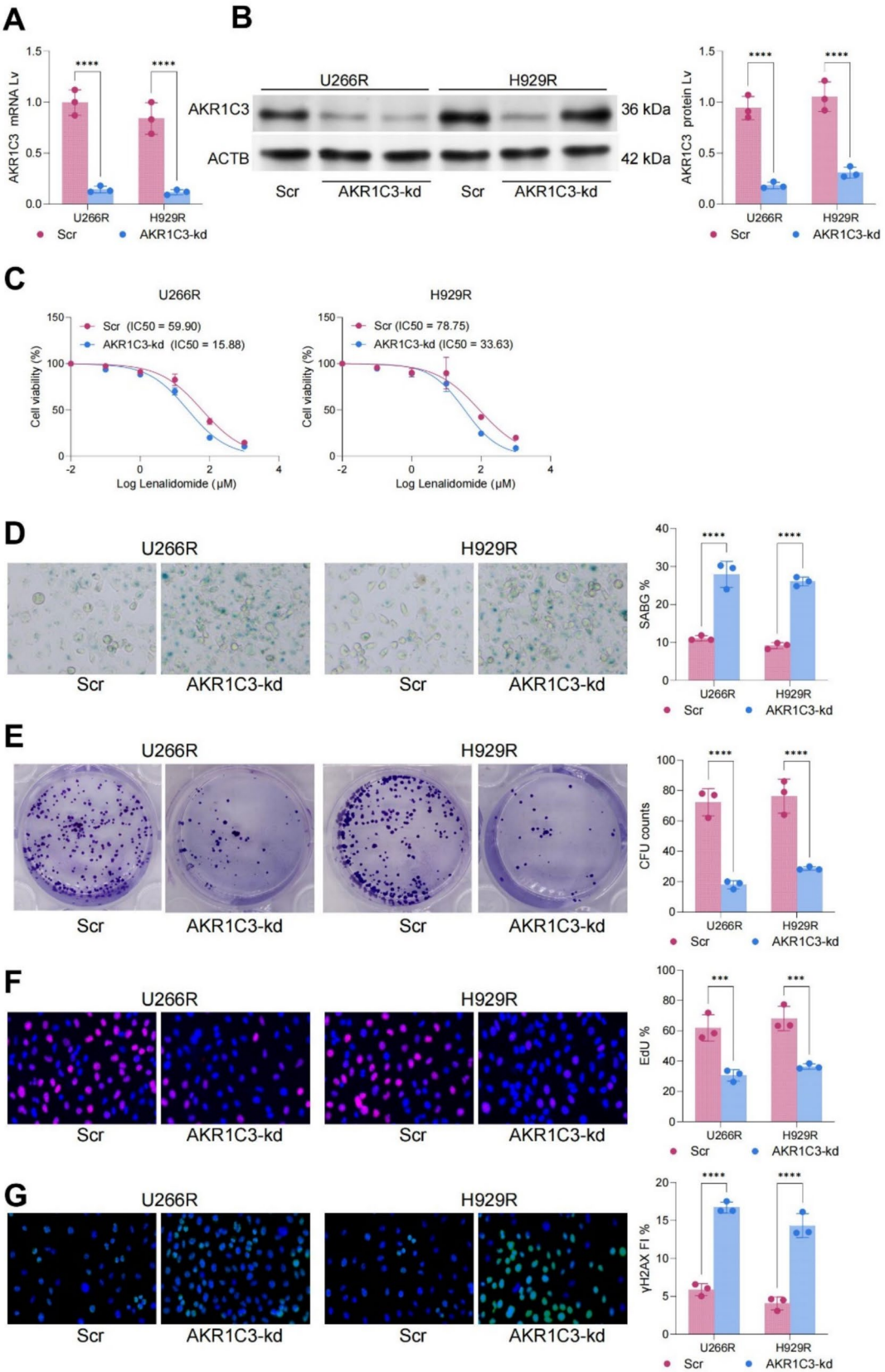
A
AKR1C3 mRNA Lv
U266R
H929R
Scr
AKR1C3-kd
B
U266R
H929R
AKR1C3
ACTB
36 kDa
42 kDa
Scr
AKR1C3-kd
AKR1C3 protein Lv
C
U266R
H929R
Scr (IC50 = 59.90)
AKR1C3-kd (IC50 = 15.88)
Scr (IC50 = 78.75)
AKR1C3-kd (IC50 = 33.63)
Cell viability (%)
Log Lenalidomide (μM)
D
SABG %
E
CFU counts
F
EdU %
G
γH2AX FI %

◂**Fig. 2** AKR1C3 knockdown enhanced LEN sensitivity in MM cells. **A** After AKR1C3 knockdown, AKR1C3 mRNA and protein levels were significantly reduced in the LEN-resistant MM cell lines H929R and U266R, as confirmed by RT−qPCR and WB analysis. (n = 3). **B** WB analysis confirming decreased AKR1C3 protein levels in H929R and U266R cells after shRNA transfection (n = 3). **C** Comparison of LEN IC_{50} values between control and AKR1C3-knockdown (AKR1C3-kd) H929R and U266R cells (n = 6). **D** SABG staining showing increased senescence in H929R and U266R cells treated with LEN (10 nM) following AKR1C3 knockdown (n = 3). **E** Colony formation assay showing reduced colony formation ability in H929R and U266R cells after AKR1C3 knockdown under LEN treatment (n = 3). **F** Cell proliferation assay showing a significant decrease in the proliferative ability of H929R and U266R cells upon AKR1C3 knockdown under LEN treatment (n = 3). **G** Immunofluorescence staining for gamma-H2AX indicating increased DNA damage in H929R and U266R cells treated with LEN following AKR1C3 knockdown (n = 3). Differences were analysed using the Student's *t* tests. The bar graphs represent the means ± SDs of independent replicate experiments. $^{**}p < 0.01$, $^{***}p < 0.001$, $^{****}p < 0.0001$

using IgG, YY1, CEBPA, and ATF4 antibodies (2 μg) (Table 3). Antibody/chromatin complexes were then captured with protein G agarose (4 °C, 2 h). After resuspension and centrifugation to collect protein/DNA complexes, protein/DNA cross-links were decrosslinked to release free DNA. Purified DNA was subjected to qPCR to quantify protein−DNA binding. The primer sequences are listed in Table 2.

Statistical analysis

Statistical analysis was conducted via Prism 8.0.2 (GraphPad). Data were collected from a minimum of three individual experiments and expressed as the mean ± standard deviation. Differences between two groups were assessed using the Student's *t* tests. Survival analysis was performed via the log-rank test, with statistical significance set at $p < 0.05$.

Results

AKR1C3 is upregulated in LEN-resistant MM cells

We mined significantly aberrantly expressed genes in MM from the GEO dataset GSE6477 (Fig. 1A). Additionally, aberrantly expressed genes in LEN-resistant MM patients were analysed via the GSE222411 dataset (Fig. 1B). Cross-referencing revealed three intersecting genes (Fig. 1C). Among them, the expression of AKR1C3, which acts as an oncogenic factor [32], showed the most prominent difference. According to the data from the GSE136324 dataset, AKR1C3 was considered to be highly expressed in MM (Fig. 1D). The data from the Cancer Genome Atlas (TCGA) revealed a significant correlation between high AKR1C3 expression and poor prognosis. All MM patients in the TCGA database received standard therapies including proteasome inhibitors (PIs), immunomodulatory drugs (IMiDs), or monoclonal antibodies (mAbs) (Fig. 1E). To verify the role of AKR1C3 in LEN resistance, we constructed the LEN-resistant MM cell lines H929 and U266 through an increasing gradient of LEN doses. Compared with the parental cell lines, these cell lines presented a significantly increased half maximal inhibitory concentration (IC_{50}) of LEN (Fig. 1F), indicating the successful generation of LEN-resistant cells, which were designated the H929R and U266R cell lines. Notably, RT−qPCR and WB revealed markedly elevated levels of the AKR1C3 mRNA and protein in LEN-resistant cells (Fig. 1G, H).

Knockdown of AKR1C3 enhances LEN sensitivity in MM cells

To confirm the role of AKR1C3 in LEN resistance in MM cells, we subsequently transfected H929R and U266R cells with shRNA targeting AKR1C3. The mRNA and protein levels of AKR1C3 decreased significantly in these cell lines (Fig. 2A, B). Notably, this transfection significantly decreased the IC_{50} of LEN in both H929R and U266R cells, indicating their weaker resistance to LEN (Fig. 2C). In subsequent experiments, H929R and U266R cells were treated with LEN at a fixed concentration (10 nM). SABG staining revealed that the senescence of both cell lines was significantly increased upon ARK1C3 knockdown (Fig. 2D). Moreover, their ability to form colonies and proliferate was impaired (Fig. 2E, F). Additionally, sh-AKR1C3 administration significantly increased the expression of gamma-H2AX in cells following LEN treatment, indicating a substantial increase in DNA damage (Fig. 2G). These results confirmed the critical role of AKR1C3 in the resistance of MM cells to LEN.

AKR1C3 knockdown interrupts metabolic reprogramming in MM cells

Recent evidence has highlighted the role of AKR1C3 in modulating glycolysis [33]. Here, we found that the levels of glycolysis-related factors, such as HK2, GLUT1 and PKM2, in LEN-resistant MM cells significantly decreased following AKR1C3 knockdown (Fig. 3A, B). Additionally, knocking down AKR1C3 in cells reduced the production of ATP and lactate (Fig. 3C, D) and glucose uptake (Fig. 3E). Furthermore, XF24 extracellular flux analysis revealed a significant decrease in the ECAR but an increase in the OCR in drug-resistant MM cells after AKR1C3 knockdown. Additionally, the ECAR and OCR of AKR1C3-knockdown LEN-resistant MM cells were similar to those of parental cells, indicating reversal of the Warburg phenotype (Fig. 3F, G). Consistent

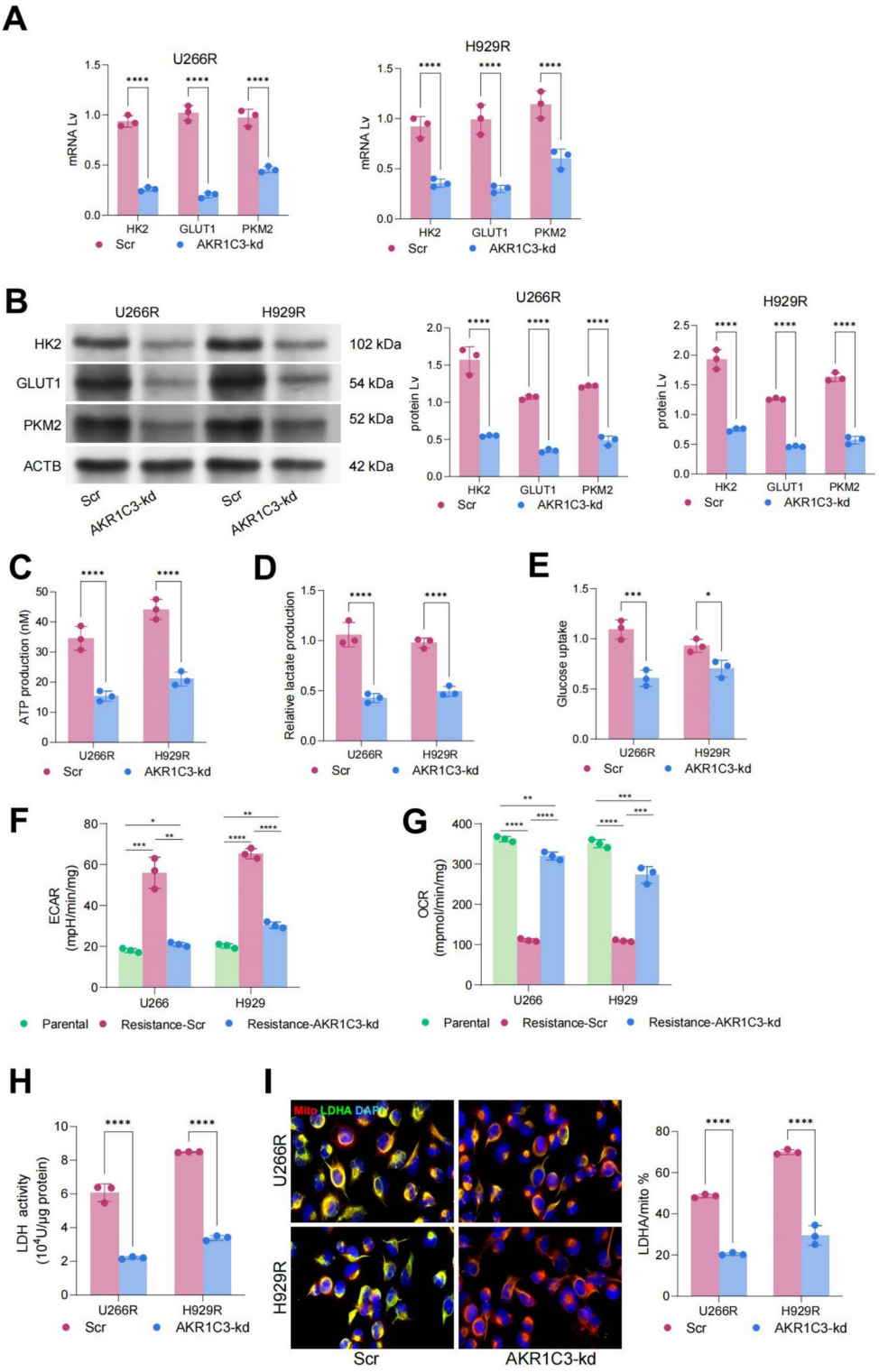

Fig. 3 AKR1C3 knockdown interrupts metabolic reprogramming in MM cells. **A**, **B** RT−qPCR and WB analysis showing decreased levels of HK2, GLUT1, and PKM2 in LEN-resistant MM cells following AKR1C3 knockdown (n = 3). **C**, **D** Quantification of ATP and lactate production in LEN-resistant MM cells, showing significant reductions after AKR1C3 knockdown (n = 3). **E** Glucose uptake assay demonstrating reduced glucose uptake in LEN-resistant MM cells upon AKR1C3 knockdown (n = 3). **F**, **G** Knockdown of AKR1C3 counteracted the increase in the ECAR and decrease in the OCR in LEN-resistant MM cells (n = 3). **H** LDH activity assay showing significantly reduced LDH activity in LEN-resistant MM cells following AKR1C3 knockdown (n = 3). **I** Immunofluorescence staining indicating a decrease in the colocalization of LDHA (green) with mitochondria (red) in LEN-resistant MM cells upon AKR1C3 knockdown. Nuclei were stained with DAPI (blue) (n = 3). Differences were analysed using the Student's *t* tests. The bar graphs present the means ± SDs of independent replicate experiments. $^{**}p < 0.01$, $^{***}p < 0.001$, $^{****}p < 0.0001$ (color figure online)

with these findings, AKR1C3 knockdown in H929R and U266R cells significantly reduced the activity of lactate dehydrogenase (LDH), an enzyme responsible for glycolysis and lactate production (Fig. 3H). Moreover, immunofluorescence staining revealed that the colocalization of LDHA with mitochondria was inhibited in AKR1C3-knockdown cells (Fig. 3I).

YY1 activates AKR1C3 transcription in MM cells

To further verify the upregulation of AKR1C3 in LEN resistance, we utilized the JASPAR website to predict transcription factors that bind to the AKR1C3 promoter. The results identified YY1, CEBPA, and ATF4 as potential binding partners (Fig. 4A). Using anti-YY1 antibodies, ChIP−qPCR revealed prominent precipitation of AKR1C3 promoter segments. Furthermore, we noted a stronger association between YY1 and the AKR1C3 promoter in LEN-resistant cells than the other two genes (Fig. 4B, C). The mRNA levels of YY1 were significantly elevated in U266R and H929R cells. Although the mRNA levels of CEBPA and ATF4 also increased in U266R or H929R cells, YY1 showed the greatest change (Fig. 4D). Consistent with these findings, the protein levels of YY1 were significantly elevated in U266R and H929R cells (Fig. 4E). Therefore, we considered YY1 to be the main regulatory factor of AKR1C3. Using the GSE136324 dataset, we observed increased expression of AKR1C3 and YY1 in the MM cells of MM patients (Fig. 4F). Through survival analysis of the MMRF-CoMMpass cohort in the TCGA database, we observed a significant correlation between high YY1 expression and poor prognosis in MM patients (Fig. 4G). Additionally, AKR1C3 was positively correlated with YY1 expression (Fig. 4H). Moreover, YY1 overexpression in parental cells significantly increased AKR1C3 expression, whereas YY1 knockdown in LEN-resistant cells markedly reduced AKR1C3 levels (Fig. 4I, J). Additionally, YY1 overexpression in parental cells led to a notable increase in the LEN IC_{50}, whereas YY1 knockdown in resistant cells resulted in a significant decrease in the LEN IC_{50} (Fig. 4K).

AKR1C3 overexpression restores LEN resistance and glycolysis in MM cells suppressed by YY1 silencing

To further explore the interaction between YY1 and AKR1C3 in LEN resistance, we silenced YY1 in U266R and H929 cells with or without AKR1C3 overexpression (Fig. 5A, B). After silencing YY1, the IC_{50} values for LEN were markedly decreased in both cell lines, yet this effect was abrogated by subsequent overexpression of AKR1C3 (Fig. 5C). Under 10 nM LEN treatment, YY1 silencing promoted the senescence of U266R and H929 cells, but their ability to form colonies and proliferate was increased. However, these changes were reversed upon AKR1C3 overexpression (Fig. 5D–F). YY1 silencing was found to reduce the ECAR while enhancing gamma-H2AX and OCR in the two cell lines, and these effects were negated by AKR1C3 overexpression (Fig. 5G–I). Furthermore, AKR1C3 overexpression restored lactate and ATP production and increased glucose consumption in H929R and U266R cells, and these changes were suppressed upon YY1 knockdown (Fig. 5J–L). Importantly, in YY1-low-expressing cells, AKR1C3 overexpression facilitated the colocalization of LDHA and mitochondria (Fig. 5M).

AKR1C3 activates the Hedgehog signalling pathway to increase LEN resistance in MM cells

To delve deeper into the downstream signalling pathways associated with AKR1C3, we conducted Kyoto Encyclopedia of Genes and Genomes (KEGG) enrichment analysis on genes from the GSE222411 dataset that presented a correlation coefficient greater than 0.3 with AKR1C3 expression. Our analysis revealed the predominant involvement of these genes in the Hedgehog, steroid hormone biosynthesis, and metabolic pathways (Fig. 6A). Previous studies have highlighted the pivotal role of the Hedgehog signalling pathway in drug resistance across various cancers [34].

Subsequently, we proved that the expression levels of key Hedgehog pathway markers (GLI1, HIP1, and PTCH1) increased significantly in LEN-resistant cells but then decreased upon AKR1C3 or YY1 knockdown. Conversely, YY1 overexpression in parental cells increased the expression of Hedgehog pathway markers (Fig. 6B, C).

Additionally, U266R and H929R cells with stable AKR1C3 knockdown were treated with the Hedgehog pathway agonist fluticasone (FTS). FTS significantly reduced the sensitivity of cells to LEN (Fig. 6D–G), accompanied by glycolytic overactivity (Fig. 6H–M).

Discussion

Beyond direct antimyeloma effects, LEN's pharmacological activity in MM involves antiangiogenic suppression, immune modulation, and remodelling of the tumour microenvironment [17]. Acquired drug resistance in MM arises through genomic instability, BM microenvironmental adaptation, ATP-binding cassette transporter upregulation, and epigenetic reprogramming [35]. Emerging evidence has delineated key pathways driving LEN resistance [16, 36]. In this study, we further revealed that YY1-mediated transcription of AKR1C3 and activation of the Hedgehog signalling pathway play critical roles in acquired LEN resistance and glycolysis in MM cells.

Our bioinformatic analysis identified AKR1C3 as an aberrantly activated gene in LEN-resistant samples. We confirmed that AKR1C3 expression was increased in LEN-resistant MM cell lines compared with parental cell lines. AKR1C3 has been well established as a tumour promoter in castration-resistant prostate cancer, where it catalyses the synthesis of active androgens to promote tumour progression [37, 38]. In addition, emerging

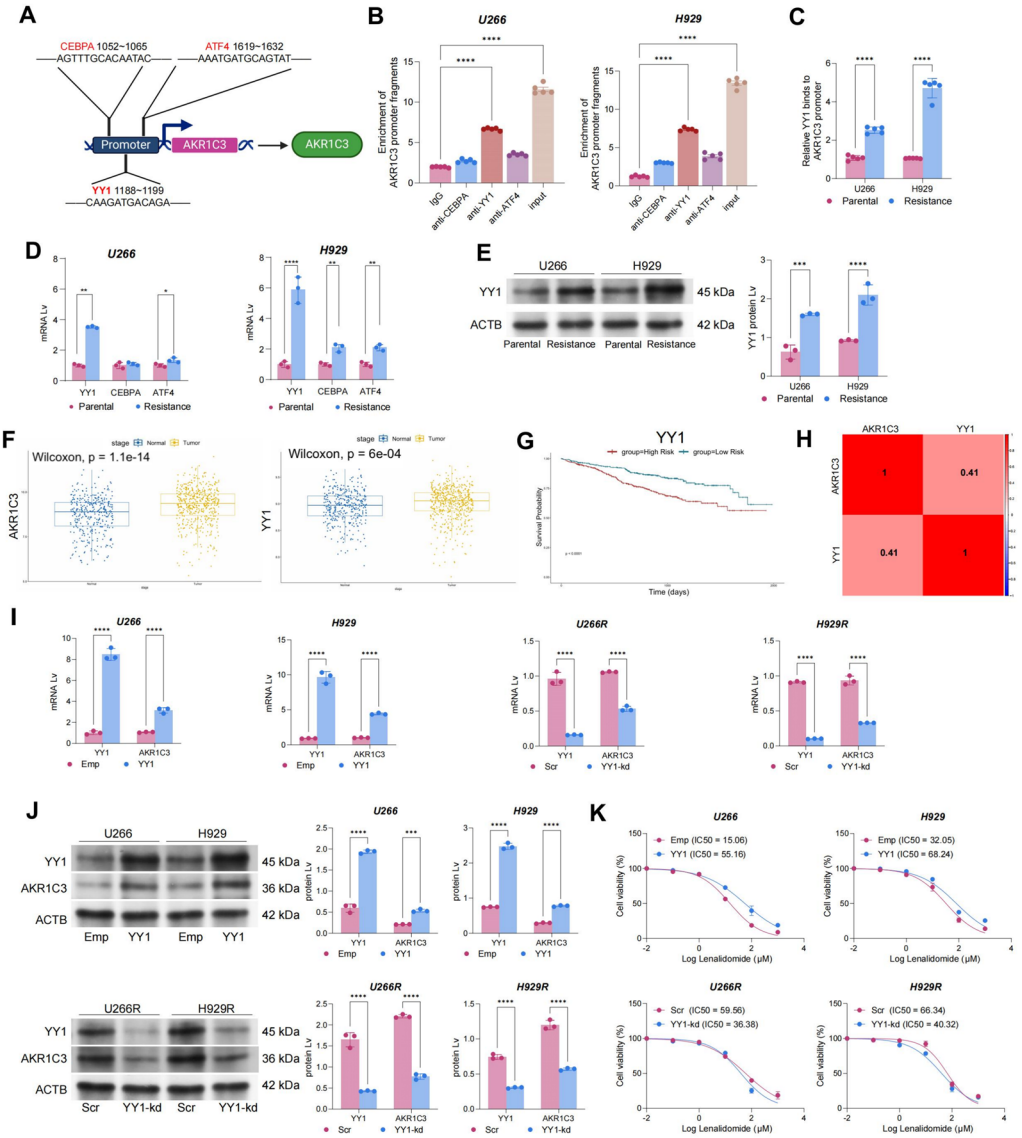

Fig. 4 YY1 activates AKR1C3 transcription. **A** Prediction of transcription factor binding to the AKR1C3 promoter via the JASPAR website, identifying YY1, CEBPA, and ATF4 as potential binding partners. **B** ChIP data showing a stronger association between YY1 and the AKR1C3 promoter than between CEPBA and ATF4 in LEN-resistant cells (n = 5). **C** ChIP showing increased precipitation of AKR1C3 promoter segments with anti-YY1 antibodies in LEN-resistant cells compared with parental cells (n = 3). **D** mRNA levels of YY1, CEBPA, and ATF4 in LEN-resistant MM cells compared with parental cells, as demonstrated by RT−qPCR analysis (n = 3). **E** WB analysis demonstrating elevated YY1 protein levels in LEN-resistant MM cells compared with parental cells (n = 3). **F** Increased expression of AKR1C3 and YY1 was observed in MM cells from Fig. 4 YY1 activates AKR1C3 tran**s**cription. A Prediction of transcription factor binding to the AKR1C3 promoter via the JASPAR website, identifying YY1, CEBPA, an**d** ATF4 as potential binding partners. B ChIP data showing a stronge**r** ass**oci**ation between YY1 and the AKR1C3 promoter than between CEPBA and ATF4 in LEN-resistant cells (n = 5). C ChIP showing inc**r**eased precipitation of AKR1C3 p**ro**moter segments with $ant_{i\text{-}Y}$Y1 antibodies in LEN-resistant cells compared with parental cells (n = 3). D mRNA levels of YY1, CEBPA, and ATF4 in LEN-resistant MM cells compared with parental cells, as demonstrated by RT–qPCR *an*alysis (n = 3). E WB analysis demonstrating elevated YY1 protein levels in LEN-resist*an*t MM cells *com*pared with pa*r*ental cells (n = *3*). F Increased expression of AKR1C3 and YY1 was observed in MM cells from MM patients in the GSE136324 dataset. G A significant correlation between high YY1 expression and poor prognosis in MM patients was detected in the GSE136324 dataset. H AKR1C3 expression was positively correlated with YY1 expression. I, J Effects of YY1 overexpression and knockdown on AKR1C3 expression in parental and LEN-resistant MM cells, as assessed by RT–qPCR and WB analysis (n = 3). K Comparison of LEN IC50 values between YY1-overexpressing parental MM cells and YY1-knockdown LEN-resistant MM cells, indicating the impact of YY1 on LEN resistance (n = 3). Differences were analysed using the Student's t tests. The bar graphs present the means ± SDs of independent replicate experiments. *p < 0.05, **p < 0.01, ***p < 0.001, ****p < 0.0001 (color figure online)

evidence has highlighted the oncogenic role of AKR1C3 in other malignancies, such as hepatocellular carcinoma [39, 40] and breast cancer [41]. Specifically, AKR1C3 has been associated with increased resistance of cancer cells to chemotherapeutics [42, 43]. In this study, we clarified the correlation between AKR1C3 and acquired LEN resistance in MM cell lines, as AKR1C3 silencing significantly reduced LEN IC_{50} values and induced cell senescence and DNA damage. In myeloma, LEN may impair DNA repair and increase the sensitivity of cells to DNA damage [44]. Studies have shown that AKR1C3 adapts hepatocellular carcinoma cells to targeted therapy by regulating lipid droplet formation and glycolysis [19]. Similarly, AKR1C3 has been reported to be correlated with autophagy-dependent glycolysis in thyroid cancer cells through the activation of extracellular signal-regulated kinase (ERK) signalling [33]. Here, we found that AKR1C3 silencing in two LEN-resistant MM cell lines reduced the ECAR but increased the OCR, resulting in low lactate production, glucose uptake, LDH release, and decreased colocalization of LDHA1 with mitochondria within cells. These findings provide direct evidence that AKR1C3 mediates metabolic reprogramming to promote the growth and LEN resistance of MM cells.

As an upstream regulator of AKR1C3, YY1 was shown to bind to the AKR1C3 promoter in MM cell lines, particularly in LEN-resistant cell lines. YY1 functions as either a transcriptional activator or repressor, depending on its cofactors [27, 28]. However, the specific cofactors with which YY1 interacts to modulate AKR1C3 transcription remain unexplored in the present study. Increased YY1 stability has been correlated with tumorigenesis in MM [45]. Yin et al. reported in 2023 that YY1 promotes the proliferation and bortezomib resistance of MM cells by interacting with the lncRNA taurine upregulated gene 1 (TUG1) and upregulating YOD1 [31]. Here, we found that YY1 silencing similarly enhanced LEN sensitivity in LEN-resistant cells, which was due, at least in part, to the upregulation of AKR1C3. These findings provide novel evidence that YY1 is correlated with increased LEN resistance in MM. YY1 increases immune resistance in tumour cells by modulating the expression of programmed cell death ligand 1 (PD-L1), an immune checkpoint point leading to T-cell exhaustion [46]. As described above, LEN exerts MM-eliminating effects partly by increasing the T-cell population and its cytotoxicity [11–13]. Therefore, YY1 may also confer LEN resistance to cells by directly modulating PD-L1 expression, which requires further investigation.

Subsequent KEGG enrichment analysis revealed the close involvement of AKR1C3-related genes in Hedgehog signalling, a key pathway associated with cell stemness and drug resistance across various cancers [34, 47, 48], including MM [49, 50]. Here, we observed that this signalling pathway, which is activated by YY1 and AKR1C3, was implicated in the acquisition of LEN resistance and the enhancement of glycolytic activity in MM cells. In addition, the Hedgehog agonist FTS restored LEN resistance and glycolysis in cells whose resistance was suppressed by AKR1C3 silencing. This evidence provides a deeper understanding of the oncogenic effects of YY1 and AKR1C3 in MM.

Emerging evidence highlights immune modulation and metabolic reprogramming as promising strategies to overcome drug resistance in MM. MM-driven metabolic remodeling fosters a hypoxic, acidic, and nutrient-deprived tumour BM microenvironment, which impairs antitumour immunity and induces angiogenesis [51]. Studies have shown that drugs targeting the glycolytic pathway can play an anti-MM role [52] and overcome drug resistance [53]. In colon cancer studies, JHU083, a compound that blocks glutamine metabolism, can suppress the Warburg effect in tumours and activate T cells [54]. Direct targeting of angiogenic cytokines/receptors has not shown good efficacy in patients with MM [55]. These underscoring the importance of combination regimens based on antitumour, antiangiogenic, and antidrug resistance agents. For instance, the combination of GANT61 and valproic acid synergistically inhibits the proliferation of multiple myeloma cells through the suppression of the Hedgehog signalling pathway [49]. The YY1-AKR1C3-Hedgehog axis we identified in LEN-resistant MM cells may provide novel biomarker and therapeutic targets for LEN-resistant MM patients. Although further research is needed to better understand resistance mechanisms, our study potentially offers a novel combination therapy for the treatment of MM.

The clinical relevance of our results could be enhanced with a longer patient follow-up period. The resistance mechanisms in MM are multifaceted, and critical aspects such as comprehensive validation of resistance persistence and evaluation of potential cross-resistance patterns among IMiDs require further systematic investigation. Here, we confirmed the role of the YY1-AKR1C3-Hedgehog axis in LEN-resistant MM cells, but further details, such as whether YY1 interacts with other elements and the specific mechanism by which the Hedgehog pathway mediates glycolysis, remain to be determined.

In conclusion, YY1 induces the transcription of AKR1C3 to activate the Hedgehog signalling pathway, thus enhancing LEN resistance and glycolytic activity in MM cells. Any member of the YY1/AKR1C3/Hedgehog

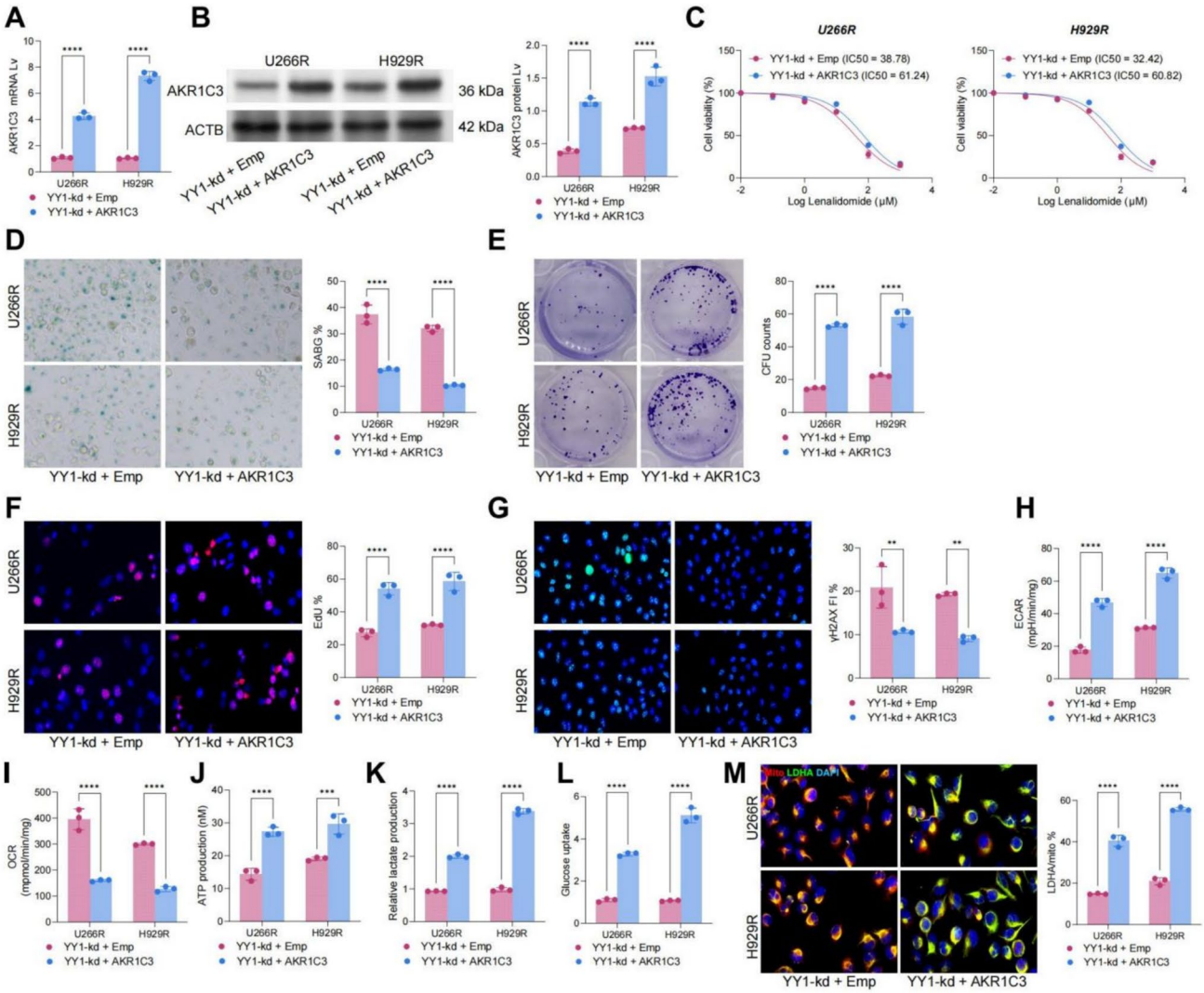

Fig. 5 AKR1C3 overexpression restores LEN resistance and glycolysis in MM cells suppressed by YY1 silencing. **A** AKR1C3 mRNA levels in H929R and U266R cells following YY1 knockdown (YY1-kd) and AKR1C3 overexpression (AKR1C3) were determined via RT−qPCR (n = 3). **B** WB confirming increased AKR1C3 protein levels in cells following YY1 knockdown and AKR1C3 overexpression (n = 3). **C** Comparison of LEN IC_{50} values in cells, as determined by the CCK-8 assay (n = 6). **D** SABG staining showing senescence in cells treated with 10 nM LEN (n = 3). **E** Colony formation ability of the cells was determined via a colony formation assay (n = 3). **F** Proliferation of cells determined via an EdU labelling assay (n = 3). **G** Immunofluorescence staining for gamma-H2AX indicating DNA damage in cells (n = 3). **H**, **I**. Assessment of the ECAR and OCR in cells (n = 3). **J** Assessment of ATP production in cells (n = 3). **K** Assessment of lactate production in cells (n = 3). **L** Assessment of glucose uptake in cells (n = 3). **M** Colocalization of LDHA (green) and mitochondria (red) in cells was analysed by immunofluorescence staining; nuclei were stained with DAPI (blue) (n = 3). Differences were analysed using the Student's *t* tests. The bar graphs present the means ± SDs of independent replicate experiments. $^{**}p < 0.01$, $^{***}p < 0.001$, $^{****}p < 0.0001$ (color figure online)

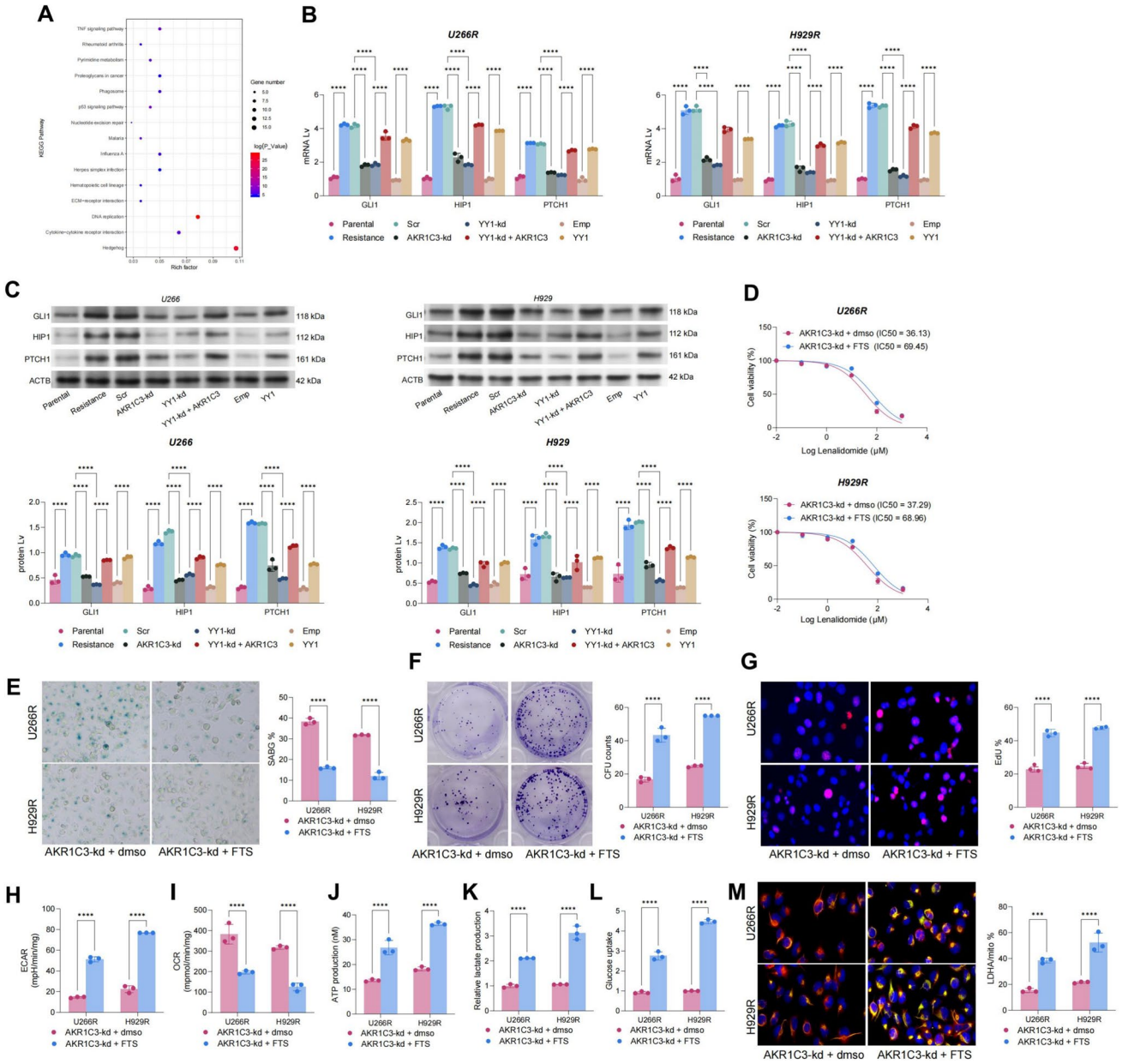

Fig. 6 AKR1C3 activates the Hedgehog signalling pathway to increase LEN resistance in MM cells. **A** KEGG enrichment analysis of genes with correlation coefficients greater than 0.3 with AKR1C3 expression in the GSE222411 dataset. **B**, **C** Detection of the mRNA and protein expression levels of key markers in the Hedgehog signalling pathway in parental and LEN-resistant cells via qPCR and WB (n = 3). **D** U266R and H929R cells with stable AKR1C3 knockdown were additionally treated with the Hedgehog pathway agonist fluticasone. LEN IC_{50} values in cells determined by the CCK-8 assay (n = 6). **E** SABG staining showing senescence in H929R and U266R cells under 10 nM LEN treatment (n = 3). **F** Colony formation ability of the cells was determined via a colony formation assay (n = 3). **G** Proliferation of cells determined via an EdU labelling assay (n = 3). **H**, **I** Assessment of the ECAR and OCR in cells (n = 3). **J** Assessment of ATP production in cells (n = 3). **K** Assessment of lactate production in cells (n = 3). **L** Assessment of glucose uptake in cells (n = 3). **M** Colocalization of LDHA (green) and mitochondria (red) in cells was analysed by immunofluorescence staining; nuclei were stained with DAPI (blue) (n = 3). Differences were analysed using the Student's *t* tests. The bar graphs present the means ± SDs of independent replicate experiments. $^{**}p < 0.01$, $^{***}p < 0.001$, $^{****}p < 0.0001$ (color figure online)

axis may be targeted to overcome LEN resistance and aberrant energy metabolism during MM progression.

Acknowledgements Not applicable.

Author contributions Yang Chen conceived and designed the experiments, performed the experiments, and drafted the manuscript. Aijia Zhang: performed the experiments and data analysis. Yuan Wang: performed the bioinformatics analysis. Daoda Qi and Chengyi Peng collected the data. Zihao Liang: performed the experiments. Jingjing Guo designed the study and supervised and supported the analysis. Yan Gu: designed the study, acquired the findings, and critically revised the manuscript. All the authors discussed the results and accepted the final version of the manuscript.

Funding Nanjing Second Hospital Talent Promotion Project,RCMS232013, Geriatric Health Research Project of Jiangsu Provincial Health Commission, LKM2022037, Key Project of Research Project of Jiangsu Provincial Health Commission, K2023018.

Data availability No datasets were generated or analysed during the current study.

Declarations

Conflict of interest The authors declare no competing interests.

Ethical approval and consent to participate Not applicable.

Consent for publication Not applicable.

References

1. Bray F, Laversanne M, Sung H, Ferlay J, Siegel RL, Soerjomataram I, Jemal A. Global cancer statistics 2022: GLOBOCAN estimates of incidence and mortality worldwide for 36 cancers in 185 countries. CA Cancer J Clin. 2024;74(3):229–63.
2. Brigle K, Rogers B. Pathobiology and diagnosis of multiple myeloma. Semin Oncol Nurs. 2017;33(3):225–36.
3. Kyle RA, Rajkumar SV. Treatment of multiple myeloma: a comprehensive review. Clin Lymphoma Myeloma. 2009;9(4):278–88.
4. Wang J, De Veirman K, Faict S, Frassanito MA, Ribatti D, Vacca A, Menu E. Multiple myeloma exosomes establish a favourable bone marrow microenvironment with enhanced angiogenesis and immunosuppression. J Pathol. 2016;239(2):162–73.
5. Ria R, Reale A, De Luisi A, Ferrucci A, Moschetta M, Vacca A. Bone marrow angiogenesis and progression in multiple myeloma. Am J Blood Res. 2011;1(1):76–89.
6. Vacca A, Ribatti D. Bone marrow angiogenesis in multiple myeloma. Leukemia. 2006;20(2):193–9.
7. Rajkumar SV, Hayman SR, Lacy MQ, Dispenzieri A, Geyer SM, Kabat B, Zeldenrust SR, Kumar S, Greipp PR, Fonseca R, et al. Combination therapy with lenalidomide plus dexamethasone (Rev/Dex) for newly diagnosed myeloma. Blood. 2005;106(13):4050–3.
8. Kumar SK, Rajkumar V, Kyle RA, van Duin M, Sonneveld P, Mateos MV, Gay F, Anderson KC. Multiple myeloma. Nat Rev Dis Primers. 2017;3:17046.
9. Noonan K, Rudraraju L, Ferguson A, Emerling A, Pasetti MF, Huff CA, Borrello I. Lenalidomide-induced immunomodulation in multiple myeloma: impact on vaccines and antitumour responses. Clin Cancer Res. 2012;18(5):1426–34.
10. Corral LG, Haslett PA, Muller GW, Chen R, Wong LM, Ocampo CJ, Patterson RT, Stirling DI, Kaplan G. Differential cytokine modulation and T cell activation by two distinct classes of thalidomide analogues that are potent inhibitors of TNF-alpha. J Immunol. 1999;163(1):380–6.
11. Davies FE, Raje N, Hideshima T, Lentzsch S, Young G, Tai YT, Lin B, Podar K, Gupta D, Chauhan D, et al. Thalidomide and immunomodulatory derivatives augment natural killer cell cytotoxicity in multiple myeloma. Blood. 2001;98(1):210–6.
12. Chang DH, Liu N, Klimek V, Hassoun H, Mazumder A, Nimer SD, Jagannath S, Dhodapkar MV. Enhancement of ligand-dependent activation of human natural killer T cells by lenalidomide: therapeutic implications. Blood. 2006;108(2):618–21.
13. Schafer PH, Gandhi AK, Loveland MA, Chen RS, Man HW, Schnetkamp PP, Wolbring G, Govinda S, Corral LG, Payvandi F, et al. Enhancement of cytokine production and AP-1 transcriptional activity in T cells by thalidomide-related immunomodulatory drugs. J Pharmacol Exp Ther. 2003;305(3):1222–32.
14. Ng YLD, Ramberger E, Bohl SR, Dolnik A, Steinebach C, Conrad T, Muller S, Popp O, Kull M, Haji M, et al. Proteomic profiling reveals CDK6 upregulation as a targetable resistance mechanism for lenalidomide in multiple myeloma. Nat Commun. 2022;13(1):1009.
15. Cohen YC, Zada M, Wang SY, Bornstein C, David E, Moshe A, Li B, Shlomi-Loubaton S, Gatt ME, Gur C, et al. Identification of resistance pathways and therapeutic targets in relapsed multiple myeloma patients through single-cell sequencing. Nat Med. 2021;27(3):491–503.
16. Kulig P, Milczarek S, Bakinowska E, Szalewska L, Baumert B, Machalinski B. Lenalidomide in multiple myeloma: review of resistance mechanisms, current treatment strategies and future perspectives. Cancers (Basel). 2023;15(3):963.
17. Li M, Zhang L, Yu J, Wang X, Cheng L, Ma Z, Chen X, Wang L, Goh BC. AKR1C3 in carcinomas: from multifaceted roles to therapeutic strategies. Front Pharmacol. 2024;15:1378292.
18. Naidansuren P, Park CW, Kim SH, Nanjidsuren T, Park JJ, Yun SJ, Sim BW, Hwang S, Kang MH, Ryu BY, et al. Molecular characterization of bovine placental and ovarian 20alpha-hydroxysteroid dehydrogenase. Reproduction. 2011;142(5):723–31.
19. Wu C, Dai C, Li X, Sun M, Chu H, Xuan Q, Yin Y, Fang C, Yang F, Jiang Z, et al. AKR1C3-dependent lipid droplet formation confers hepatocellular carcinoma cell adaptability to targeted therapy. Theranostics. 2022;12(18):7681–98.
20. Navarro C, Ortega A, Santeliz R, Garrido B, Chacin M, Galban N, Vera I, De Sanctis JB, Bermudez V. Metabolic reprogramming in cancer cells: emerging molecular mechanisms and novel therapeutic approaches. Pharmaceutics. 2022;14(6):1303.

21. Liberti MV, Locasale JW. The Warburg effect: how does it benefit cancer cells? Trends Biochem Sci. 2016;41(3):211–8.
22. Schwartz L, Supuran CT, Alfarouk KO. The Warburg effect and the hallmarks of cancer. Anticancer Agents Med Chem. 2017;17(2):164–70.
23. Sancho P, Barneda D, Heeschen C. Hallmarks of cancer stem cell metabolism. Br J Cancer. 2016;114(12):1305–12.
24. Icard P, Shulman S, Farhat D, Steyaert JM, Alifano M, Lincet H. How the Warburg effect supports aggressiveness and drug resistance of cancer cells? Drug Resist Updat. 2018;38:1–11.
25. Gavriatopoulou M, Paschou SA, Ntanasis-Stathopoulos I, Dimopoulos MA. Metabolic disorders in multiple myeloma. Int J Mol Sci. 2021;22(21):11430.
26. Gaston K, Fried M. YY1 is involved in the regulation of the bi-directional promoter of the Surf-1 and Surf-2 genes. FEBS Lett. 1994;347(2–3):289–94.
27. Verheul TCJ, van Hijfte L, Perenthaler E, Barakat TS. The why of YY1: mechanisms of transcriptional regulation by Yin Yang 1. Front Cell Dev Biol. 2020;8: 592164.
28. Peng PH, Chen JL, Wu HH, Yang WH, Lin LJ, Lai JC, Chang JS, Syu JL, Wu HT, Hsu FT, et al. Interplay between lncRNA RP11–367G18.1 variant 2 and YY1 plays a vital role in hypoxia-mediated gene expression and tumourigenesis. Cancer Cell Int. 2023;23(1):266.
29. Guo AM, Sun K, Su X, Wang H, Sun H. YY1TargetDB: an integral information resource for Yin Yang 1 target loci. Database (Oxford). 2013;2013:bat007.
30. Jung M, Bui I, Bonavida B. Role of YY1 in the regulation of anti-apoptotic gene products in drug-resistant cancer cells. Cancers (Basel). 2023;15(17):4267.
31. Yin Q, Shen X, Xu H, Feng W, Shi X, Ju S. YY1-induced LncRNA-TUG1 elevates YOD1 to promote cell proliferation and inhibit bortezomib sensitivity in multiple myeloma. Leuk Lymphoma. 2023;64(6):1161–74.
32. Liu Y, He S, Chen Y, Liu Y, Feng F, Liu W, Guo Q, Zhao L, Sun H. Overview of AKR1C3: inhibitor achievements and disease insights. J Med Chem. 2020;63(20):11305–29.
33. Gao Y, Tao W, Wang S, Duan R, Zhang Z. AKR1C3 silencing inhibits autophagy-dependent glycolysis in thyroid cancer cells by inactivating ERK signaling. Drug Dev Res. 2024;85(1):e22142.
34. Nguyen NM, Cho J. Hedgehog pathway inhibitors as targeted cancer therapy and strategies to overcome drug resistance. Int J Mol Sci. 2022;23(3):1733.
35. Robak P, Drozdz I, Szemraj J, Robak T. Drug resistance in multiple myeloma. Cancer Treat Rev. 2018;70:199–208.
36. Osada N, Kikuchi J, Iha H, Yasui H, Ikeda S, Takahashi N, Furukawa Y. c-FOS is an integral component of the IKZF1 transactivator complex and mediates lenalidomide resistance in multiple myeloma. Clin Transl Med. 2023;13(8): e1364.
37. Endo S, Oguri H, Segawa J, Kawai M, Hu D, Xia S, Okada T, Irie K, Fujii S, Gouda H, et al. Development of novel AKR1C3 inhibitors as new potential treatment for castration-resistant prostate cancer. J Med Chem. 2020;63(18):10396–411.
38. Hertzog JR, Zhang Z, Bignan G, Connolly PJ, Heindl JE, Janetopoulos CJ, Rupnow BA, McDevitt TM. AKR1C3 mediates pan-AR antagonist resistance in castration-resistant prostate cancer. Prostate. 2020;80(14):1223–32.
39. Zhou Q, Tian W, Jiang Z, Huang T, Ge C, Liu T, Zhao F, Chen T, Cui Y, Li H, et al. A positive feedback loop of AKR1C3-mediated activation of NF-kappaB and STAT3 facilitates proliferation and metastasis in hepatocellular carcinoma. Cancer Res. 2021;81(5):1361–74.
40. Chen J, Zhang J, Tian W, Ge C, Su Y, Li J, Tian H. AKR1C3 suppresses ferroptosis in hepatocellular carcinoma through regulation of YAP/SLC7A11 signaling pathway. Mol Carcinog. 2023;62(6):833–44.
41. Liu Y, Chen Y, Jiang J, Chu X, Guo Q, Zhao L, Feng F, Liu W, Zhang X, He S, et al. Development of highly potent and specific AKR1C3 inhibitors to restore the chemosensitivity of drug-resistant breast cancer. Eur J Med Chem. 2023;247: 115013.
42. He S, Chu X, Wu Y, Jiang J, Fang P, Chen Y, Liu Y, Qiu Z, Xiao Y, Li Z, et al. Development of biaryl-containing aldo-keto reductase 1C3 (AKR1C3) inhibitors for reversing AKR1C3-mediated drug resistance in cancer treatment. J Med Chem. 2023;66(14):9537–60.
43. Li Y, Tang J, Li J, Du Y, Bai F, Yang L, Li X, Jin X, Wang T. ARID3A promotes the chemosensitivity of colon cancer by inhibiting AKR1C3. Cell Biol Int. 2022;46(6):965–75.
44. Liu M, Zhang Y, Wu Y, Jin J, Cao Y, Fang Z, Geng L, Yang L, Yu M, Bu Z, et al. IKZF1 selectively enhances homologous recombination repair by interacting with CtIP and USP7 in multiple myeloma. Int J Biol Sci. 2022;18(6):2515–26.
45. Che F, Ye X, Wang Y, Wang X, Ma S, Tan Y, Mao Y, Luo Z. METTL3 facilitates multiple myeloma tumourigenesis by enhancing YY1 stability and pri-microRNA-27 maturation in m(6) A-dependent manner. Cell Biol Toxicol. 2023;39(5):2033–50.
46. Hays E, Bonavida B. YY1 regulates cancer cell immune resistance by modulating PD-L1 expression. Drug Resist Updat. 2019;43:10–28.
47. Giroux-Leprieur E, Costantini A, Ding VW, He B. Hedgehog signaling in lung cancer: from oncogenesis to cancer treatment resistance. Int J Mol Sci. 2018;19(9):2835.
48. Ma L, Wang Y, Chen P, Wu S. A review of Hedgehog signaling in radioresistant esophageal cancer: potential treatment target. Technol Cancer Res Treat. 2023;22:15330338231169872.
49. Zhang Z, Zhang R, Hao C, Pei X, Li J, Wang L. GANT61 and valproic acid synergistically inhibited multiple myeloma cell proliferation via hedgehog signaling pathway. Med Sci Monit. 2020;26: e920541.
50. Zhang Y, Yao G, Yang X, Qiu T, Wang S. Mechanism of targeting the hedgehog signaling pathway against chemotherapeutic resistance in multiple myeloma. J Oncol. 2022;2022:1399697.
51. Wu S, Kuang H, Ke J, Pi M, Yang DH. Metabolic reprogramming induces immune cell dysfunction in the tumour microenvironment of multiple myeloma. Front Oncol. 2020;10: 591342.
52. Fan T, Sun G, Sun X, Zhao L, Zhong R, Peng Y. Tumour energy metabolism and potential of 3-bromopyruvate as an inhibitor of aerobic glycolysis: implications in tumour treatment. Cancers (Basel). 2019;11(3):317.
53. Dalva-Aydemir S, Bajpai R, Martinez M, Adekola KU, Kandela I, Wei C, Singhal S, Koblinski JE, Raje NS, Rosen ST, et al. Targeting the metabolic plasticity of multiple myeloma with FDA-approved ritonavir and metformin. Clin Cancer Res. 2015;21(5):1161–71.
54. Leone RD, Zhao L, Englert JM, Sun IM, Oh MH, Sun IH, Arwood ML, Bettencourt IA, Patel CH, Wen J, et al. Glutamine blockade induces divergent metabolic programs to overcome tumour immune evasion. Science. 2019;366(6468):1013–21.
55. Saltarella I, Altamura C, Campanale C, Laghetti P, Vacca A, Frassanito MA, Desaphy JF. Anti-angiogenic activity of drugs in multiple myeloma. Cancers (Basel). 2023;15(7):1990.